ACS OMEGA

http://pubs.acs.org/journal/acsodf

Article

Surface Coating of Titanium Dioxide Nanoparticles with a Polymerizable Chelating Agent and Its Physicochemical Property

NaRi Kim, Yerin Kim, Je-Moon Yun, Soon-Kyu Jeong, Sulhae Lee, Beom Zoo Lee, and Jongwon Shim*

Cite This: *ACS Omega* 2023, 8, 18743−18750

Read Online

ACCESS | Metrics & More | Article Recommendations | Supporting Information

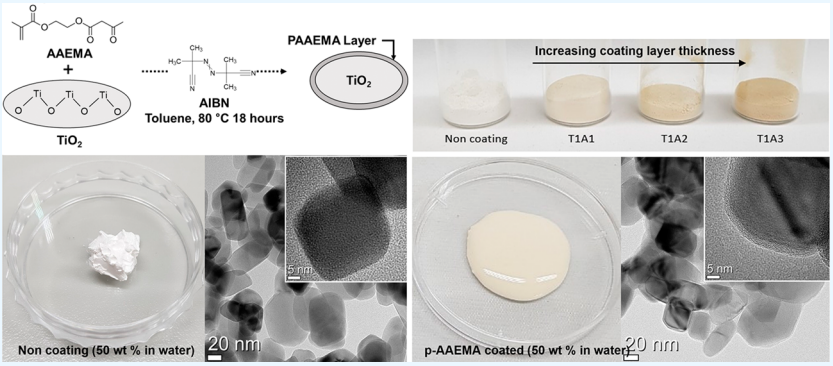

ABSTRACT: Surface modification of inorganic nanoparticles is critical for the quality and performance of pigments, cosmetics, and composite materials. We covered the titanium dioxide nanoparticles' surface with 2-(acetoacetoxy) ethyl methacrylate, a polymerizable chelating agent. Through the in situ polymerization procedure, this molecule's β-ketoester moiety quickly coordinated with the metal atoms on titanium dioxide nanoparticles, and its methacrylate group formed homogeneous coating layers. This coating layer significantly reduced the photocatalytic activity of titanium dioxide nanoparticles and prevented their aggregation. This nanoparticle dispersion showed low viscosity up to the solid content of 60% (w/w) in the liquid dispersant. As a result, it increased the UV screening performance and dispersion stability. Additionally, this coating layer widened the absorption spectrum of titanium dioxide and could change the color of nanoparticles from pale yellow to brown. It can also be helpful for cosmetic applications.

1. INTRODUCTION

The annual production of inorganic sunscreen agents, such as titanium dioxide and zinc oxide, according to the exposure increment of ultraviolet wavelength to the earth's surface, has been increasing for decades.[1,2] Among those, titanium dioxide nanoparticles (TiO_2 NPs) have been most widely utilized as an ultraviolet wavelength (UV) screening material to prevent photodegradation of various commercial products, including polymers, textile, paint, personal care products, and cosmetics.[1−8] However, the strong aggregation and sedimentation properties make TiO_2 NPs hard to disperse and stabilize in dispersing media with high content.[9−11] Furthermore, the high level of the chemical potential can make TiO_2 NPs produce reactive oxygen species (ROS) under UV irradiation. Generated hydroxy radicals and superoxide anions can induce inflammatory responses and degradation of lipid molecules in the skin tissue.[12,13] Therefore, modulation of surface properties of TiO_2 NPs for ensuring dispersion stability and safety is a significant issue for making consumer products.

Instead of surface modification, using surfactants and polymers as physical stabilizers in dispersion media can retard the creation of nanoparticle aggregates and increase dispersion viscosity. However, the feed ratio of stabilizers vastly increases proportionally to the TiO_2 NP amount and their size distribution, wherein a higher stabilizer content tends to lower the solid content of the dispersion.[14,15] Similarly, the UV screening performance of inorganic nanoparticles, represented as a sun screening protection factor (SPF), is affected by nanoparticle dispersion stability.[16,17] Therefore, a large portion of surfactants and stabilizers is inevitably used for cosmetic formulations, but they also can lower skin texture and irritate the skin.[18,19]

ROS cause the deterioration of proteins, lipids, and even DNA and disturb cell signaling.[20,21] In previous studies, encapsulating TiO_2 NPs with silica or polymethylmethacrylate (PMMA) has been suggested to reduce ROS generation and enhance dispersion stability in liquid media. Although the optical property of PMMA and silica did not lower the UV

Received: February 4, 2023
Accepted: April 28, 2023
Published: May 15, 2023

screening effect of TiO_2 NPs and could reduce the generation of ROS,[1,22] conformal surface coating of inert TiO_2 NPs without binding molecules is still challenging. Moreover, it was reported that a high ROS generation level was detected from silica-alumina-coated TiO_2 NPs.[23,24]

Therefore, this report introduced a newly developed nanothickness dense polymer coating method on the TiO_2 NPs. 2-(acetoacetoxy)ethyl methacrylate (AAEMA). It can make low viscous nanoparticle dispersion at a high solid content with minimized ROS generation without additional binding molecules. AAEMA is a polymerizable chelating agent molecule with a reactive methylene moiety and a ketoester chelating group. It has been used to make copolymers with acylates and styrene and to crosslink in adhesives and sealants.[25,26] Unlike the nonspecific adhesion of dopamine, the adhesion property of AAEMA is site-specific like other natural metal-chelating agents, polyphenols.[27,28] After radical polymerization, the AAEMA polymer (p-AAEMA) can be postcrosslinked at room temperature via ketoester groups. It can enhance the weatherability, hydrolytic stability, and low water absorbency of a copolymer.[29] However, we utilized ketoester groups of AAEMA monomer molecules to make a strong coordination bond onto the TiO_2 NP surface, and it can be polymerized as a conformal coating layer by a batch process. This coordination-polymerization procedure is a facile way to form a conformal coating layer onto various metal oxide nanoparticles. Rheological properties of p-AAEMA-coated TiO_2 NPs, optical characteristics, and sun protection factor values were also evaluated for topical applications.

2. RESULTS AND DISCUSSION

2.1. Synthesis and Characterization. As described in schematic illustration (Scheme 1), the β-ketoester group of

Scheme 1. Illustration of p-AAEMA Coating on TiO_2 Nanoparticles

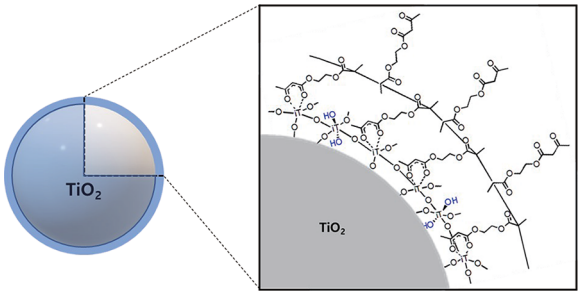

AAEMA molecules can form a coordination bond with a titanium atom on TiO_2 NPs. The other reactive group of this monomer, ethyl methacrylate, can readily be polymerized.[32] When the bare TiO_2 NPs dispersed in toluene were mixed with AAEMA at room temperature, the color changed instantly from white to pale yellow or light brown. This characteristic chelating color represents the chelation of AAEMA monomers with titanium atoms.[33] We examined various organic solvents as reaction media. Because the monomer adsorption kinetic on TiO_2 NPs in solvents follows the Freundlich adsorption isotherm, high AAEMA miscibility in a solvent decreases adsorption onto the TiO_2 NP surface.[34,35] As shown in Figure S1a, the color of TiO_2 NPs and AAEMA (computational log $P_{o/w}$ = 0.8) mixture in polar aprotic and protic media such as methanol (log $P_{o/w}$ = −0.74), ethyl acetate (log $P_{o/w}$ = 0.7), and ethanol (log $P_{o/w}$ = 0.24) showed a weak intensity. In comparison, it showed strong color intensity in nonpolar media such as toluene (log $P_{o/w}$ = 2.8) and xylene (log $P_{o/w}$ = 3.0). We also could get higher production yield when we used nonpolar solvents (Figure S1b). Therefore, we determined that the AAEMA monomer solubility of dispersion media affected the thickness of coating layers after polymerization.

2.2. FT-IR Analysis. The FT-IR absorption spectra of the bare TiO_2 NPs, pure AAEMA monomers, and their mixture are shown in Figure 1a. After monomer mixing with bare TiO_2,

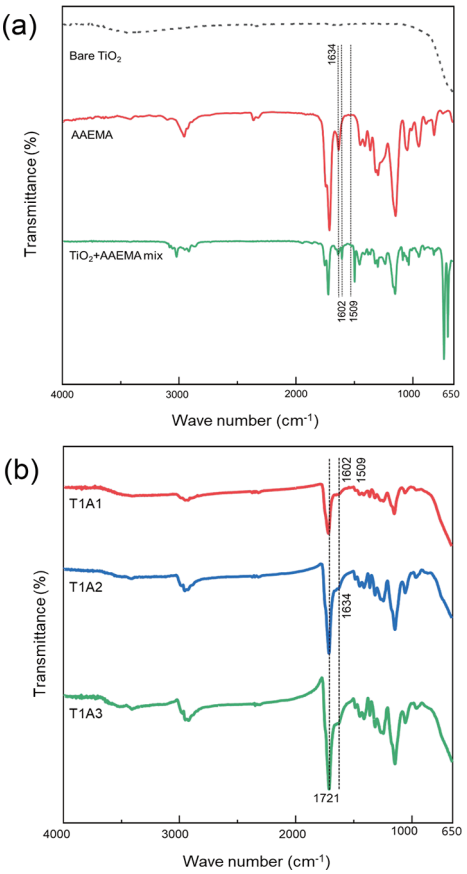

Figure 1. (a) FT-IR spectrum of bare TiO_2 NPs and the AAEMA monomer, (b) FT-IR spectrum of p-AAEMA-coated samples with varied monomer feed ratios (T1A1, T1A2, and T1A3).

two peaks appeared at 1602 and 1509 cm^{-1}. They are ascribed to the band of stretching vibrations of ν (C═O) and ν (C═C) of the enolic form of the β-ketoesters bridged to titanium atoms.[36] After polymerization, the distinctive ν (C═C, methacrylate) peak of the AAEMA monomer almost disappeared at a wavelength of 1634 cm^{-1}. As the feed ratio of the AAEMA monomer increased, the absorption band near 1721 cm^{-1}, which is assigned to the carbonyl groups (C═O, stretching), gradually increased (Figure 1b).[37−39]

2.3. Thermal Degradation Analysis. Thermogravimetric analysis (TGA) determined the coating amount of p-AAEMA on TiO_2 nanoparticles under nitrogen. Thermograms of p-AAEMA-coated TiO_2 nanoparticles (T1A1, T1A2, T1A3) and bare TiO_2 nanoparticles are shown in Figure 2a. The expected maximum weight loss of p-AAEMA in surface-coated TiO_2 nanoparticles with a monomer-to-nanoparticle feed ratio of 1/1 (T1A1) was about 6.5 wt %, and 1/2 (T1A2), 1/3 (T1A3) samples were 30 and 35 wt %. On the other hand, the weight

https://doi.org/10.1021/acsomega.3c00734
ACS Omega 2023, 8, 18743−18750

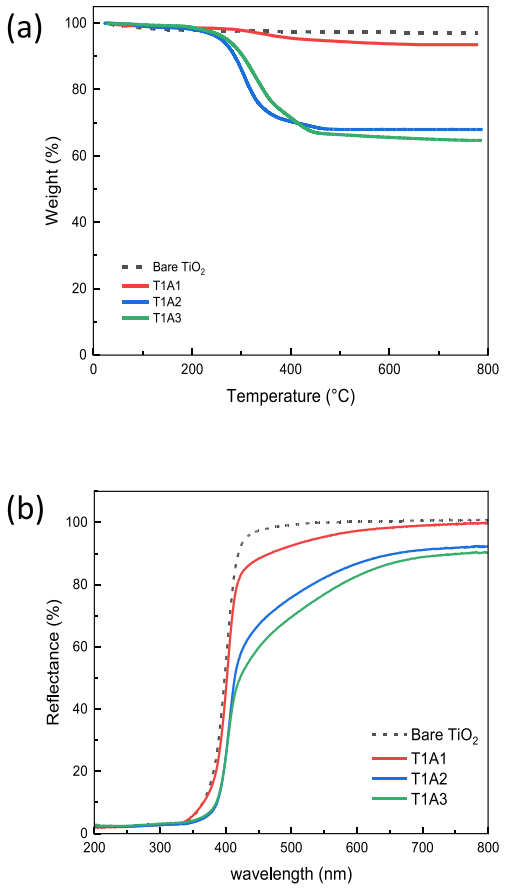

Figure 2. (a) TGA thermogram and (b) diffuse reflectance of bare TiO_2 and p-AAEMA-coated samples with monomer feed ratios (T1A1, T1A2, and T1A3).

loss of bare TiO_2 nanoparticles was 2.9% by weight. Therefore, we determined that the p-AAEMA coating amount was not linearly proportional to the feeding amount of the AAEMA monomer. As shown in Figure S2, we found a few p-AAEMA-coated TiO_2 NP aggregates at the bottom of the reactor at feed ratios 1/2 and 1/3. It was suspected that an excess amount of AAEMA in the solvent could induce nanoparticular aggregation during polymerization.

2.4. Diffuse Reflectance Analysis. In Figure S1c, the color of p-AAEMA-coated TiO_2 NPs was graded according to the monomer feed ratio to TiO_2 NPs. Figure 2b shows the diffuse reflectance spectra of p-AAEMA-coated TiO_2 NPs samples with given monomer feed ratios. Compared to bare TiO_2 NPs, the diffuse reflectance of these surface-coated NPs indicated a significant decrease in blue and green wavelength absorption. We suspected that this reflection decrease of the 400−550 nm band is due to charge transfer via ligand-to-metal coordination formation.[40] The UV−vis absorption peak of the AAEMA monomer is located below 300 nm (Figure S3), and the amount of AAEMA could not consistently impact the absorption of 400 to 550 nm of p-AAEMA-coated TiO_2 NPs.

2.5. Photocatalytic Activity. When exposed to UV light, the reactive oxygen species generated by titanium dioxide nanoparticles can damage cells and tissues by their photocatalytic property. It is controlled by various factors such as particle size, surface area, crystal structure, and surface properties.[41,43] In most cases, surface treatment, including polymer encapsulation, can enhance dispersion stability and biocompatibility, but photocatalytic activity is also stabilized or enhanced by preventing particle aggregation.[44,45] However, the p-AAEMA coating surface resisted oxygen radical generation and particle aggregation.

The amount of hydroxy radical generated by the rutile phase TiO_2 NPs under UV light was measured by terephthalic acid assay. The fluorescent emission peak around 430 nm for 2-hydroxyterephthalic acid indicated the concentration of hydroxy radicals. As shown in Figure 3a, the bare TiO_2 NPs

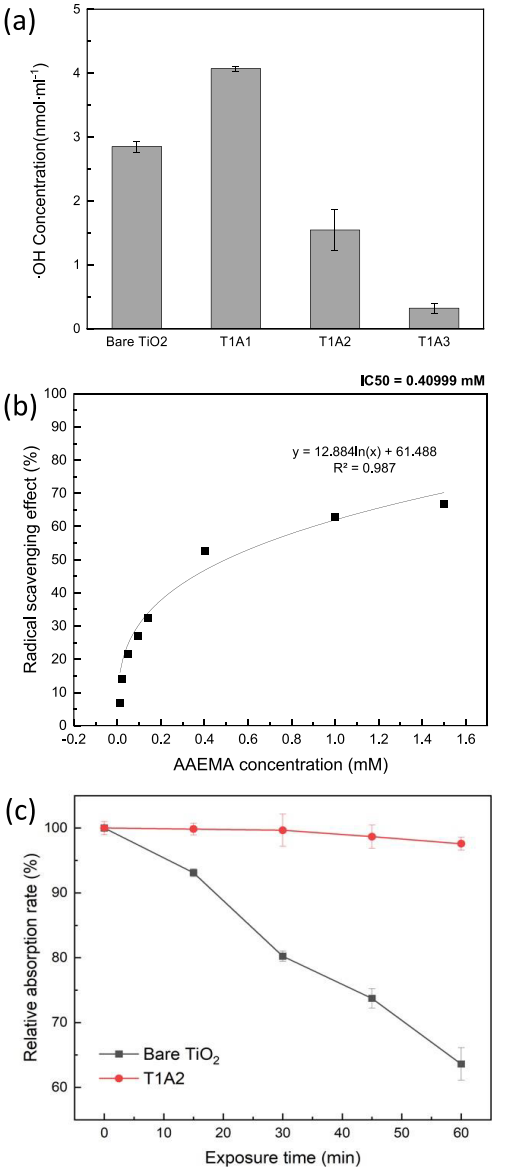

Figure 3. (a) Hydroxy radical concentration of bare TiO2 NPs and p-AAEMA-coated TiO2 NPs with varied feed ratios. (b) Radical scavenging efficiency of the AAEMA monomer. (c) Photocatalytic degradation of methylene blue.

generated hydroxy radicals at a concentration of 2.8 ± 0.08 nmol mL^{-1}, but p- AAEMA-coated TiO_2 NPs (T1A1) showed an increased radical amount at a concentration of 4.07 ± 0.04 nmol mL^{-1}. In comparison, T1A2 and T1A3 having a thicker coating p-AAEMA layer suppressed radical generation at a concentration of 1.5 ± 0.31 nmol mL^{-1} for T1A2 and 0.3 ± 0.07 nmol mL^{-1} for T1A3. The increase of radical generation by T1A1 can be due to the widening of the absorption

https://doi.org/10.1021/acsomega.3c00734
ACS Omega 2023, 8, 18743−18750

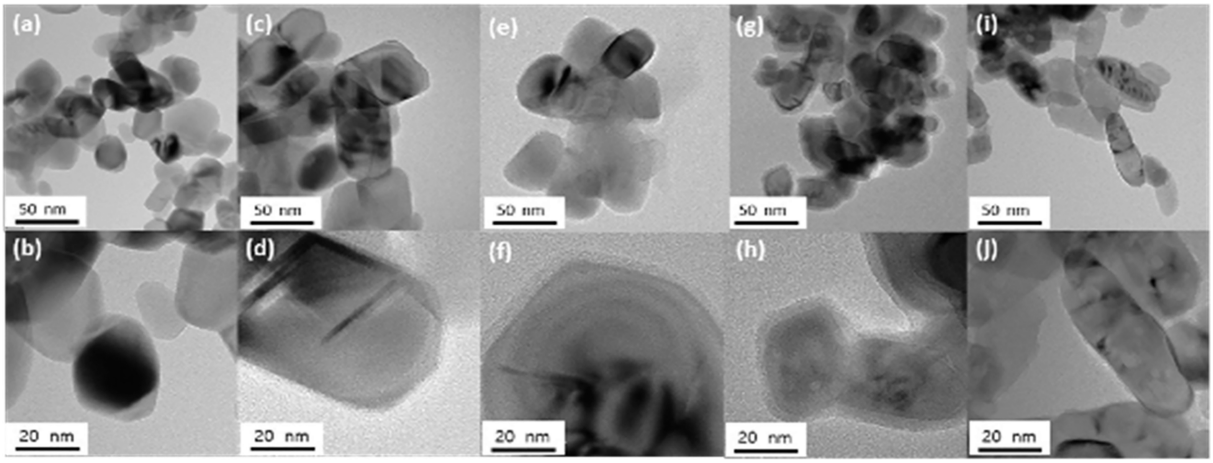

Figure 4. TEM images of bare TiO_2 NPs (a, b) and p-AAEMA-coated TiO_2 NPs with varied feed ratios. T1A1 (c, d), T1A2 (e, f), and T1A3 (g, h). Commercial TiO_2 NPs (ST-485SA15) coated with aluminum hydroxide and stearic acid (i, j).

spectrum of ligand−metal charge transfer (LCST) via the coordination of AAEMA and titanium atoms.[40]

On the contrary, the significantly lowered radical amount of T1A2 and T1A3 was due to the free β-ketoester moieties within the p-AAEMA coating layer. The radical scavenging effect of β-ketoester groups was previously reported in other research studies.[41] We also confirmed the radical scavenging activity of the AAEMA monomer by DPPH absorbance with IC_{50} of 0.41 mM in Figure 3b. In addition, because the absorption of p-AAEMA-coated TiO_2 NPs around 400 nm can affect the absorption intensity of 2-hydroxyterephthalic acid, we examined the photocatalytic activity of the surface-coated TiO_2 NPs (T1A2) comparing with the bare TiO_2 with methylene blue (Figure 3c). As a result, the absorption intensity of MB with bare TiO_2 NPs decreased rapidly under UV irradiation, but p-AAEMA-coated TiO_2 NPs scarcely lowered. We also confirmed that the AAEMA monomer's absorption did not change MB's absorption intensity with and without UV exposure (Figure S4). As a result, we could determine a critical amount of p-AAEMA coating that can reduce the radical generation of TiO_2 NPs under UV irradiation.

2.6. Transmission Electron Microscopy. p-AAEMA coating via titanium atoms could be more efficient against surface modification via hydroxyl groups with a coupling agent. Chien-Hou et al. reported that the density of surface hydroxyl groups of commercial TiO_2 NPs (Degussa P25, Ishihara ST-01) was 4.8∼5.3/nm^2 by TGA analysis.[42] Although the hydroxyl group density of TiO_2 NPs differs by their crystalline phase, the average number of surface titanium atoms outnumbers the number of terminal hydroxyl groups. As shown in Figure 4, the p-AAEMA could get high coverage of the TiO_2 NP surface (Figure 4c−h) compared with the coating layer morphology of aluminum hydroxide and fatty acid on commercial TiO_2 NPs (Figure 4i,j). This coating layer's thickness varied from 1.5 to 5.5 nm along with a monomer to nanoparticle mixing ratio (wt/wt). A higher monomer feeding ratio produced thicker coating layers.

2.7. Rheological Study. *2.7.1. Particle Size Stability.* The average particle size of p-AAEMA-coated TiO_2 NPs (T1A1, T1A2, T1A3) and bare TiO_2 NPs samples dispersed in DI water at pH = 10 was measured once every four days by dynamic light scattering analysis. The average particle size of bare TiO_2 NPs significantly increased than that of p-AAEMA coated ones (Figure 5a). Because β-ketoester groups of the p-

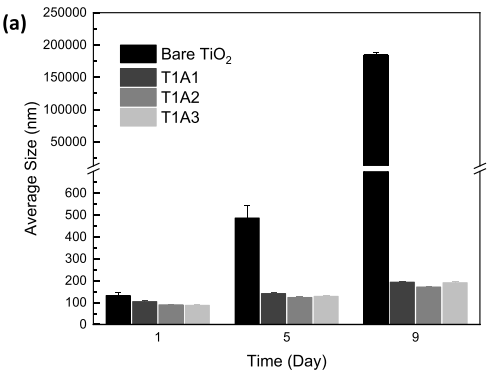

(b)

Sample	Bare TiO_2	T1A1	T1A2	T1A3
Zeta potential (mV)	-26.43	-37.82	-41.52	-45.37

Figure 5. Average particle size change with time (a) and the surface charge of TiO_2 NP samples in DI water (pH = 10) (b).

AAEMA can be easily protonated at basic conditions, surface charges of p-AAEMA-covered TiO_2 NPs were much higher than bare ones (Figure 5b). It is also helpful to utilize a typical polyacrylate thickener for cosmetic formulations because this highly negatively charged coating layer can reduce the strong interaction of TiO_2 nanoparticles with polymer chains (Figure S5).

2.7.2. Dispersion Stability. The dispersion stability of the bare TiO_2 NPs and p-AAEMA coated NPs dispersed in a squalane and 1,3-butylene glycol was monitored for 24 h by Turbiscan. Nanoparticle aggregation and sedimentation rate can be evaluated by transmission and backscattering differences in sample dispersions. As illustrated in Figure 6a,e, bare TiO_2 NP dispersion transmission progressively increased for 24 h in both solvents, representing fast settlement of NPs. Figure 6b,f also shows the rapid increase of bare TiO_2 NP dispersion backscattering due to the significant particle aggregation. In comparison, the transmission of p-AAEMA-coated nanoparticle dispersion was hardly changed in both

https://doi.org/10.1021/acsomega.3c00734
ACS Omega 2023, 8, 18743−18750

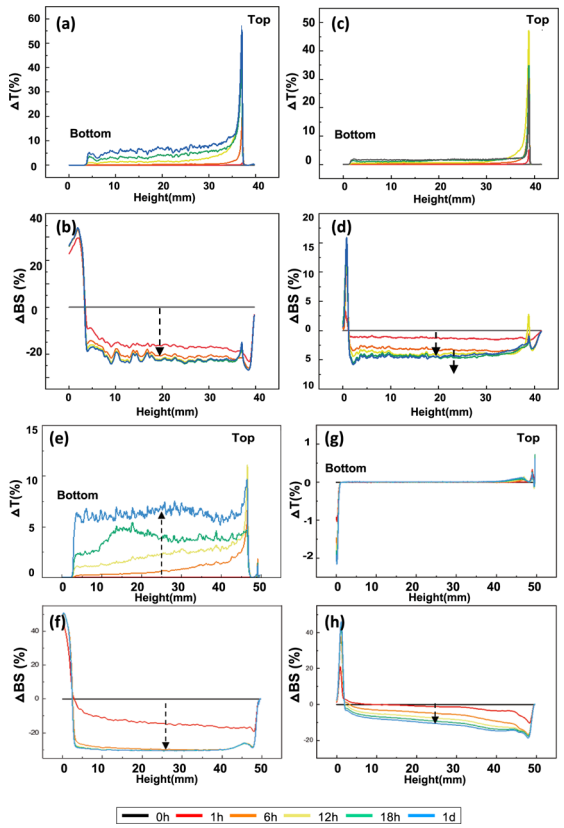

Figure 6. Transmittance and backscattering profile differences of TiO2 NP (0.5%) dispersions with time. Bare TiO_2 NPs (a, b) and p-AAEMA coated NPs (c, d) in squalane. Bare TiO2 nanoparticles (e, f) and p-AAEMA-coated TiO2 NPs (g, h) in 1, 3 butylene glycol.

media (Figure 7c,g), and the increase of backscattering was also decelerated (Figure 7d,h). Due to the viscosity difference of the dispersion medium, the sedimentation and aggregation

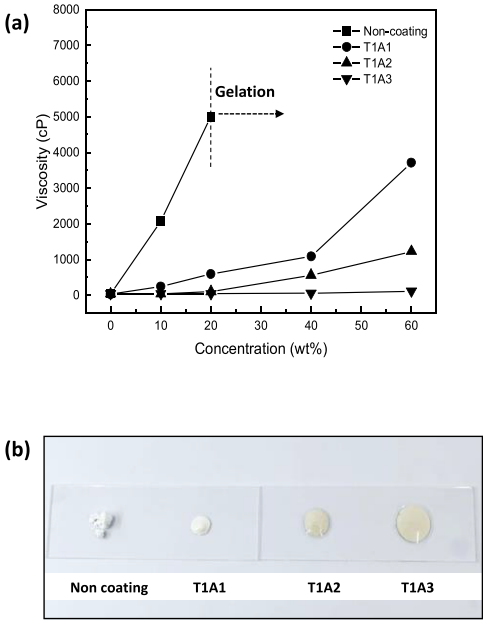

Figure 7. (a) Viscosity of bare TiO_2 NPs and p-AAEMA-coated NP dispersion in hydrocarbon oil (squalane) at various concentrations. (b) Spreadability of surface-coated TiO2 NP dispersions.

rate of bare TiO_2 NPs was much slower in squalane than in 1,3-butylene glycol.

2.7.3. Dispersion Viscosity. The viscosity of bare TiO_2 NPs and surface-coated NP samples dispersed in a saturated hydrocarbon oil (squalane) was measured at 10, 20, 40, and 60% solid contents. Above the 20 percent of solid content, bare TiO_2 NP dispersion viscosity sharply increased, forming a colloidal gel network. In comparison, the viscosity of p-AAEMA coated TiO_2 NP dispersion samples marginally changed along with solid content increase. At 60% of solid content, T1A1 dispersion showed around 4000 cps, and T1A2 and T1A3 samples showed much lower viscosity (Figure 6a). The spreadability of surface-coated TiO_2 NP dispersions also increased along with NPs' surface coating amount (Figure 6b).

2.8. Sun Protection Factor. The SPF values of T1A1 NPs dispersed in squalane as hydrophobic media and 1, 3 butylene glycol as hydrophilic liquid media are presented in Figure 8. It

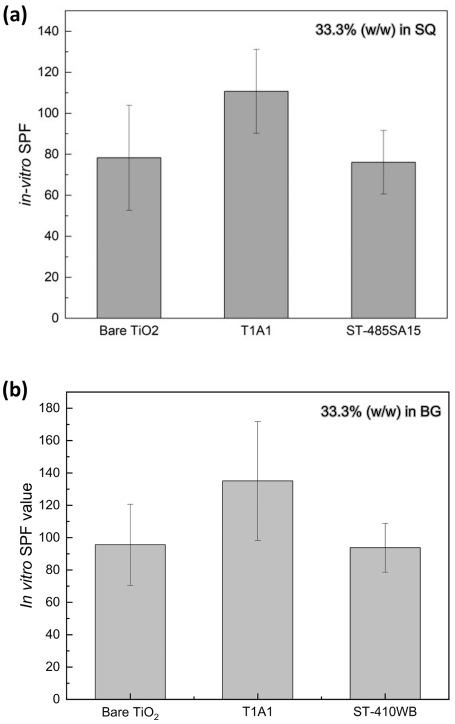

Figure 8. In vitro SPFs of TiO_2 NPs samples; (a) p-AAEMA-coated TiO2 NPs dispersed in squalene (SQ) and (b) in 1,3 butylene glycol (BG), compared with bare TiO2 NPs and commercial TiO2 NPs coated with stearic acid (ST-485SA15), and aluminum hydroxide (ST-410WB).

showed a higher SPF value of 110 ± 25 in squalane and 135 ± 36 in 1,3-butylene glycol than that of the bare TiO2 NP dispersion samples (78 ± 25 in squalane and 95 ± 25 in 1,3-butylene glycol) at the same solid content of 33%. In comparison, commercial TiO2 NPs (ST-485SA15 in squalane, ST-410WB in 1,3-butylene glycol) of which surface modified with stearic acid and aluminum hydroxide showed similar SPF values (76 ± 15 in squalane, 93 ± 15 in 1,3-butylene glycol) to the bare ones.

3. CONCLUSIONS

We synthesized a nanothickness organic uniform coating layer on bare TiO_2 NPs using a facile batch process with a polymerizable chelating agent, AAEMA, capable of instant

https://doi.org/10.1021/acsomega.3c00734
ACS Omega 2023, 8, 18743−18750

coordination and in situ polymerization. This surface coating resulted in high cosmetics and pigment industry processibility, fulfilling high dispersion stability and low viscosity of TiO_2 NPs in polar and nonpolar dispersants without additional stabilizers, even at over 50% solid content. Furthermore, the radical scavenging effect caused by plenty of catechol-like moieties in the coating layer prevents oxygen radical generation, reducing the photocatalytic toxicity of TiO_2 NPs. This negatively charged coating layer can also prevent electrostatic aggregation with conventional polyacrylate thickeners and increases the absorption of visible green and blue light, thereby reducing white cast and applying for various skin tone corrections. However, although this coating layer effectively prevents nanoparticle aggregation, the sedimentation of these high-density nanoparticles in low-viscosity media could not be completely prevented. We suspect that this coating efficiently reduces the interaction between the TiO_2 nanoparticles, but it could also reduce the interaction between the particle and dispersant molecules. Therefore, the attraction between the particle and dispersant molecule needs to be increased in further study.

4. METHODS

4.1. Materials. Rutile-phase titanium(IV) oxide nanopowder (100 nm average size range, 99.5% purity) and anatase-phase titanium(IV) oxide nanopowder (25 nm average size range, 99.7% purity) were both purchased from Sigma-Aldrich (USA). Rutile-type commercial titanium dioxide pigment nanopowder (ST-485SA15, 30∼150 nm size, Titan Kogyo, Ltd., Japan) was donated by CHEMILAND (Gyeonggi-do, Korea). 2-(Acetoacetoxy) ethyl methacrylate (AAEMA, 95% purity), 2,2′-azobisisobutyronitrile (AIBN), methylene blue, citric acid, and potassium hydroxide were purchased from Sigma-Aldrich (St. Louis, MO, USA). Squalane was purchased from Kishimoto Special Liver Oil co., Ltd. (Japan), and all analytical-grade organic solvents were purchased from Daejung Chemical (Gyeonggi-do, Korea).

4.2. Synthesis of the p-AAEMA Coating Layer. Bare TiO_2 NPs and AAEMA monomer mixture samples were prepared with defined TiO_2 and AAEMA weight ratios of 1:1 (T1A1), 1:2 (T1A2), and 1:3 (T1A3). Typically, 5 g of AAMEA monomer was dissolved in 50 mL of toluene by a sonication bath (Bransonic CPXH, Emerson, USA) for 15 min. Then, 5 g of bare TiO_2 NPs were dispersed in a monomer-toluene solution, and coordination of AAMEA monomer onto TiO_2 NPs was carried out under sonication for 1 h. Before temperature elevation, these sample mixtures were purged with nitrogen gas under agitation for 1 h at ambient temperature. Then in the presence of AIBN (0.02 mol/L), an in situ polymerization was performed for 6 h at 80 °C with stirring at 500 rpm by a multifunctional reactor system (Carousel 6 Plus reaction station, Radleys, UK). After polymerization, the surface-coated TiO_2 NPs were settled down by centrifugation at 8000 rpm and washed three times with ethanol, and dried under ambient conditions for 24 h. Before characterization, all powder samples were finely ground using an agate mortar and pestle.

4.3. Characteristics. Fourier-transform infrared spectroscopy (FT-IR, FT/IR-4200, JASCO) analysis was performed to identify the p-AAEMA coating layer on TiO_2 NPs. FT-IR spectra were collected at wavelengths between 650 and 4000 cm^{-1} wave numbers. The amounts of p-AAEMA coating on TiO_2 NPs were quantified using thermogravimetry (TGA, SDT Q600, TA Instruments, USA) at a heating rate of 20 °C min^{-1} in air under nitrogen flow 50 mL/min. The optical property of p-AAEMA-coated TiO_2 NPs was measured by diffuse reflectance spectrum analysis using a spectrophotometer (Cary 500, Agilent, USA), and the color of each powder sample was measured using a colorimeter (3nh technology, NR60CP, China). Morphology of the bare TiO_2 NPs and p-AAEMA coated NPs (T1A1, T1A2, and T1A3) was identified using a transmission electron microscope (Tecnai F20, FEI, USA) at a 20 kV of acceleration voltage. Each sample was prepared by dipping the carbon grid into a nanoparticle-dispersed water droplet.

4.4. Hydroxy Radical Analysis. The terephthalic acid assay measured hydroxy radical generated TiO_2 NPs under UV irradiation. 100 mM terephthalic acid was dissolved in 0.4 M NaOH. 0.5 mL of sample solutions having 50 mg mL^{-1} p-AAEMA-coated TiO_2 NPs were mixed with the same volume of 100 mM terephthalic acid solution and compared with bare TiO_2 NPs. Each sample was exposed under a UV lamp (8 W) for 20 min with magnetic stirring. The fluorescence intensity of the UV-irradiated dispersion samples was measured by a Microplate reader (Synergy HT, BioTek, USA) at 360 nm excitation and 400 nm emission wavelength. Pure 2-hydroxyterephthalic acid was used for making a calibration curve of hydroxy radical concentration.

4.5. Radical Scavenging Activity. The radical scavenging activity of AAEMA was measured according to the method of Blois.[30] 1 mL of AAEMA was added to 3 mL of a DPPH solution (0.2 mM in methanol). The decrease in the solution absorbance was measured at 517 nm. The percentage of DPPH radical scavenging activity was calculated using eq 1:

$$\text{Radical scavenging effect (\%)} = \left(A_0 - \frac{A_1}{A_0}\right) \times 100 \quad (1)$$

where A_0 is the absorbance of the control, and A_1 is the absorbance of samples.

4.6. Photocatalytic Activity. The photocatalytic activities of the p-AAEMA-coated anatase phase of TiO_2 NPs were investigated by observing the degradation of methylene blue (MB) under UV light.[31] 0.4 g of surface-modified TiO_2 NPs was added into 160 mL of methylene blue solution (20 ppm), and sonication was carried out for 10 min. Then, under the irradiation of cross-positioned four UV lamps (254 nm, 8 W, VILBER, France) at a 10 cm distance from the center point, 1 mL sample solution was taken out every 15 min for 1 h under magnetic stirring. The collected sample suspensions were centrifuged for 3 min at 12,000 rpm before performing the absorption measurement at 664 nm by UV−vis spectroscopy (OPTIZEN, Mecasys co LTD., Korea). The concentration of MB in the supernatant solution was calculated according to the following equation by Lambert−Beer's law.

$$\text{Relative absortion ratio (\%)} = \frac{C}{C_0} \times 100 = \frac{A_1}{A_0} \times 100 \quad (2)$$

C_0 is the MB concentration before UV exposure, and C is the concentration obtained from each sample after UV irradiation. Absorbance before UV radiation is A_0, and after radiation is A_1 at a given time.

4.7. Dispersion Stability Analysis. The dispersion properties of the p-AAEMA-coated TiO_2 NPs were compared with those of the bare TiO_2 NPs in liquid media. The viscosity

https://doi.org/10.1021/acsomega.3c00734
ACS Omega 2023, 8, 18743−18750

of the p-AAEMA-coated TiO_2 NP dispersion and the bare TiO_2 NP dispersion at 10, 20, 40, and 60% (w/w) of concentration in hydrophobic liquid media, squalane without any additional stabilizers was measured using a Brookfield RH viscometer at 20 rpm and 25 °C. The average particle size and zeta potential were measured using a dynamic light scattering analyzer (ELSZ-2000ZS, Otsuka Electronics, Japan). The concentration of the nanoparticle dispersion samples for size and zeta potential measurements was 0.01% (w/w), and they were dispersed in DI water by ultrasonication. The average size distribution of each sample was measured once a day, three times at four-day intervals, and these zeta potential values of the surface-modified nanoparticles were measured at a pH value of 10. The sedimentation and aggregation of p-AAEMA-coated TiO_2 NPs (1 wt %) dispersed in hydrophilic liquid media, 1, 3-butylene glycol were investigated using a dispersion stability analyzer (Turbiscan Lab, Formulation, USA). Delta transmission and backscattering profiles at 880 nm wavelength were obtained once an hour for 24 h.

4.8. Sun Protection Factor. in-vitro SPF values were measured using an in vitro sunscreen analyzer (UV-290AS, Pro-Lite, UK). The suspension sample preparation was followed as per ISO 24443:2012. A 33 mg nanoparticle suspension, having 33 wt % of p-AAEMA coated TiO_2 NPs in squalane and 1, 3-butylene glycol, was evenly spread on a sandblasted PMMA plate (47 × 47 × 1.5 mm, HELIO plate HD6, France), and the average transmittance of UV irradiation ($n = 6$) was measured from 290 to 400 nm at a step of 1 nm. Collected data were analyzed by the analysis of variance test and a significance level was $p < 0.05$.

■ ASSOCIATED CONTENT

Supporting Information

The Supporting Information is available free of charge at https://pubs.acs.org/doi/10.1021/acsomega.3c00734.

The color intensity of TiO_2 NPs and AAEMA mixture in organic solvents, particle aggregation formation during polymerization, UV−vis absorption spectrum of AAEMA monomer in ethanol and diffuse reflectance of surface-coated NPs, relative UV absorption of methylene blue with AAEMA monomer, and photographs of p-AAEMA-coated TiO_2 NPs and bare TiO_2 NPs mixed with a polyacrylate thickener (PDF)

■ AUTHOR INFORMATION

Corresponding Author

Jongwon Shim − *Department of Chemistry, Dongduk Women's University, Seoul 02748, Korea;* orcid.org/0000-0001-9181-5261; Email: blueray@dongduk.ac.kr

Authors

NaRi Kim − *Department of Chemistry, Dongduk Women's University, Seoul 02748, Korea*

Yerin Kim − *Department of Chemistry, Dongduk Women's University, Seoul 02748, Korea*

Je-Moon Yun − *Division of Advanced Materials Engineering, Dong-Eui University, Busan 47340, Korea*

Soon-Kyu Jeong − *R & D Team, CHEMLAND, Gunpo 15850, Korea*

Sulhae Lee − *R & D Team, CHEMLAND, Gunpo 15850, Korea*

Beom Zoo Lee − *R & D Team, CHEMLAND, Gunpo 15850, Korea*

Complete contact information is available at: https://pubs.acs.org/10.1021/acsomega.3c00734

Author Contributions

The manuscript was written through the contributions of all authors. All authors have given approval to the final version of the manuscript. J.-M.Y. contributed equally.

Notes

The authors declare no competing financial interest.

■ ACKNOWLEDGMENTS

This work was supported by the Technology Development Program (S2911008), funded by the Ministry of SMEs and Startups (MSS, Korea).

■ REFERENCES

(1) Veronovski, N.; Lešnik, M.; Lubej, A.; Verhovšek, D. Surface Treated Titanium Dioxide Nanoparticles as Inorganic UV Filters in Sunscreen Products. *Acta Chim. Slov.* **2014**, *61*, 595−600.

(2) Nakayama, N.; Hayashi, T. Preparation of TiO_2 Nanoparticles Surface-Modified by Both Carboxylic Acid and Amine: Dispersibility and Stabilization in Organic Solvents. *Colloids Surf. A Physicochem. Eng. Asp.* **2008**, *317*, 543−550.

(3) Eda, G.; Fanchini, G.; Chhowalla, M. Large-Area Ultrathin Films of Reduced Graphene Oxide as a Transparent and Flexible Electronic Material. *Nat. Nanotechnol.* **2008**, *3*, 270−274.

(4) Xia, Y.; Yang, P.; Sun, Y.; Wu, Y.; Mayers, B.; Gates, B.; Yin, Y.; Kim, F.; Yan, H. One-Dimensional Nanostructures: Synthesis, Characterization, and Applications. *Adv. Mater.* **2003**, *15*, 353−389.

(5) Jun, Y. W.; Huh, Y. M.; Choi, J. S.; Lee, J. H.; Song, H. T.; Kim, S.; Yoon, S.; Kim, K. S.; Shin, J. S.; Suh, J. S.; Cheon, J. Nanoscale Size Effect of Magnetic Nanocrystals and Their Utilization for Cancer Diagnosis via Magnetic Resonance Imaging. *J. Am. Chem. Soc.* **2005**, *127*, 5732−5733.

(6) Dick, K.; Dhanasekaran, T.; Zhang, Z.; Meisel, D. Size-Dependent Melting of Silica-Encapsulated Gold Nanoparticles. *J. Am. Chem. Soc.* **2002**, *124*, 2312−2317.

(7) Tang, Y.; Cai, R.; Cao, D.; Kong, X.; Lu, Y. Photocatalytic Production of Hydroxyl Radicals by Commercial TiO_2 Nanoparticles and Phototoxic Hazard Identification. *Toxicology* **2018**, *406-407*, 1−8.

(8) Fakin, D.; Kleinschek, K. S.; Ojstršek, A. The Role of TiO_2 Nanoparticles on the UV Protection Ability and Hydrophilicity of Polyamide Fabrics. *Acta Phys. Pol. A* **2015**, *127*, 943−946.

(9) Wu, W.; Zhang, L.; Zhai, X. Preparation and Photocatalytic Activity Analysis of Nanometer TiO_2 Modified by Surfactant. *Nanomater. Nanotechnol.* **2018**, *8*, 1−8.

(10) Fytianos, G.; Rahdar, A.; Kyzas, G. Z. Nanomaterials in Cosmetics: Recent Updates. *Nanomaterials (Basel)* **2020**, *10*, 979.

(11) Bergstrom, L. Hamaker Constants of Inorganic Materials. *Adv. Colloid Interface Sci.* **1987**, *70*, 125−169.

(12) Lee, H. J.; Park, Y. G.; Lee, S. H.; Park, J. H. Photocatalytic Properties of TiO_2 According to Manufacturing Method. *Korean Chem. Eng. Res.* **2018**, *56*, 156−161.

(13) Nasikhudin; Diantoro, M.; Kusumaatmaja, A.; Triyana, K. Study on Photocatalytic Properties of TiO_2 Nanoparticle in Various PH Condition. *J. Phys. Conf. Ser.* **2018**, *1011*, No. 012069.

(14) French, R. A.; Jacobson, A. R.; Kim, B.; Isley, S. L.; Penn, R. L.; Baveye, P. C. Influence of Ionic Strength, PH, and Cation Valence on Aggregation Kinetics of Titanium Dioxide Nanoparticles. *Environ. Sci. Technol.* **2009**, *43*, 1354−1359.

(15) Studart, R.; Amstad, E.; Gauckler, L. J. Colloidal Stabilization of Nanoparticles in Concentrated Suspensions. *Langmuir* **2007**, *23*, 1081−1090.

(16) Salameh, S.; Schneider, J.; Laube, J.; Alessandrini, A.; Facci, P.; Seo, J. W.; Ciacchi, L. C.; Mädler, L. Adhesion Mechanisms of the Contact Interface of TiO_2 Nanoparticles in Films and Aggregates. *Langmuir* **2012**, *28*, 11457−11464.
(17) Muniz-Miranda, F.; Minei, P.; Contiero, L.; Labat, F.; Ciofini, I.; Adamo, C.; Bellina, F.; Pucci, A. Aggregation Effects on Pigment Coatings: Pigment Red 179 as a Case Study. *ACS Omega* **2019**, *4*, 20315−20323.
(18) Mastrorilli, P.; Dellanna, M. M.; Rizzuti, A.; Mali, M.; Zapparoli, M.; Leonelli, C. Resin-Immobilized Palladium Nanoparticle Catalysts for Organic Reactions in Aqueous Media: Morphological Aspects. *Molecules* **2015**, *20*, 18661−18684.
(19) Mastrorilli, P.; Nobile, C. F.; Suranna, G. P.; Taurino, M. R.; Latronico, M. Synthesis and Copolymerization of a Ruthenium(II) Complex with the Deprotonated Form of 2-(Acetoacetoxy)-Ethylmetacrylate. *Inorg. Chim. Acta* **2002**, *335*, 107−112.
(20) Ono, Y.; Iwahashi, H. Titanium Dioxide Nanoparticles Impart Protection from Ultraviolet Irradiation to Fermenting Yeast Cells. *Biochem. Biophys. Rep.* **2022**, *30*, No. 101221.
(21) Dunford, R.; Salinaro, A.; Cai, L.; Serpone, N.; Horikoshi, S.; Hidaka, H.; Knowland, J. Chemical Oxidation and DNA Damage Catalysed by Inorganic Sunscreen Ingredients. *FEBS Lett.* **1997**, *418*, 87−90.
(22) Egerton, T. A. The Influence of Surface Alumina and Silica on the Photocatalytic Degradation of Organic Pollutants. *Catalysts* **2013**, *3*, 338−362.
(23) Ortelli, S.; Costa, A. L.; Matteucci, P.; Miller, M. R.; Blosi, M.; Gardini, D.; Tofail, S. A. M.; Tran, L.; Tonelli, D.; Poland, C. A. Silica Modification of Titania Nanoparticles Enhances Photocatalytic Production of Reactive Oxygen Species without Increasing Toxicity Potential in Vitro. *RSC Adv.* **2018**, *8*, 40369−40377.
(24) Kamiya, H.; Iijima, M. Surface Modification and Characterization for Dispersion Stability of Inorganic Nanometer-Scaled Particles in Liquid Media. *Sci. Technol. Adv. Mater.* **2010**, *11*, No. 044304.
(25) Dell'Anna, M. M.; Mastrorilli, P.; Rizzuti, A.; Suranna, G. P.; Nobile, C. F. Synthesis and Copolymerization of Rhodium(I) and Palladium(II) Complexes with the Deprotonated Form of 2-(Acetoacetoxy)Ethyl Methacrylate. *Inorg. Chim. Acta* **2000**, *304*, 21−25.
(26) Cui, X.; Zhu, G.; Pan, Y.; Shao, Q.; Zhao, C. X.; Dong, M.; Zhang, Y.; Guo, Z. Polydimethylsiloxane-titania nanocomposite coating: Fabrication and corrosion resistance. *Polymer* **2018**, *138*, 203−210.
(27) Sloop, J. C.; Bumgardner, C. L.; Washington, G.; Loehle, W. D.; Sankar, S. S.; Lewis, A. B. Keto-Enol and Enol-Enol Tautomerism in Trifluoromethyl-β-Diketones. *J. Fluor. Chem.* **2006**, *127*, 780−786.
(28) Iglesias, E. Tautomerization of 2-Acetylcyclohexanone. 1. Characterization of Keto-Enol/Enolate Equilibria and Reaction Rates in Water. *J. Org. Chem.* **2003**, *68*, 2680−2688.
(29) Kim, T. K.; Lee, M. N.; Lee, S. H.; Park, Y. C.; Jung, C. K.; Boo, J. H. Development of Surface Coating Technology of TiO_2 Powder and Improvement of Photocatalytic Activity by Surface Modification. *Thin Solid Films* **2005**, *475*, 171−177.
(30) Blois, M. Antioxidant Determination by Use of a Stable Free Radical. *Nature* **1958**, *181*, 1199−1200.
(31) Kim, D. S.; Han, S. J.; Kwak, S. Y. Synthesis and Photocatalytic Activity of Mesoporous TiO_2 with the Surface Area, Crystallite Size, and Pore Size. *J. Colloid Interface Sci.* **2007**, *316*, 85−91.
(32) Boyko, V.; Pich, A.; Lu, Y.; Richter, S.; Arndt, K. F.; Adler, H. J. P. Thermo-Sensitive Poly(N-Vinylcaprolactam-Co-Acetoacetoxyethyl Methacrylate) Microgels: 1 - Synthesis and Characterization. *Polymer (Guildf)* **2003**, *44*, 7821−7827.
(33) Schwartz, J.; Bernasek, S. L. Organometallic Chemistry at the Interface with Materials Science. *Catal. Today* **2001**, *66*, 3−13.
(34) Vadahanambi, S.; Lee, S.-H.; Kim, W.-J.; Oh, I.-K. Arsenic Removal from Contaminated Water Using Three-Dimensional Graphene-Carbon Nanotube-Iron Oxide Nanostructures. *Environ. Sci. Technol.* **2013**, *47*, 10510−10517.
(35) Dowaidar, A. M.; El-Shahawi, M. S.; Ashour, I. Adsorption of Polycyclic Aromatic Hydrocarbons onto Activated Carbon from Non-Aqueous Media: 1. the Influence of the Organic Solvent Polarity. *Sep. Sci. Technol.* **2007**, *42*, 3609−3622.
(36) Hoebbel, D.; Reinert, T.; Schmidt, H.; Arpac, E. On the Hydrolytic Stability of Organic Ligands in Al-, Ti- and Zr-Alkoxide Complexes. *J. Sol-Gel Sci. Technol.* **1997**, *10*, 115−126.
(37) Fotoohi, F.; Salimi, A.; Bouhendi, H.; Kabiri, K. Investigation of the Mechanical and Thermal Properties of Reactive AAEM-Co-MMA Adhesive. *Polym. Bull.* **2020**, *77*, 5767.
(38) Pavia, D. L.; Lampman, G. M.; Kriz, G. S.; Vyvyan, J. R. *Introduction to Spectroscopy*; 2008.
(39) Pal, S.; Das, A.; Maiti, S.; De, P. Synthesis and Characterization of a Biodegradable Polymer Prepared via Radical Copolymerization of 2-(Acetoacetoxy)Ethyl Methacrylate and Molecular Oxygen. *Polym. Chem.* **2012**, *3*, 182−189.
(40) Zhang, G.; Kim, G.; Choi, W. Visible Light Driven Photocatalysis Mediated via Ligand-to-Metal Charge Transfer (LMCT): An Alternative Approach to Solar Activation of Titania. *Energy Environ. Sci.* **2014**, *7*, 954−966.
(41) He, Y.; Peng, G.; Jiang, Y.; Zhao, M.; Wang, X.; Chen, M.; Lin, S. Environmental Hazard Potential of Nano-Photocatalysts Determined by Nano-Bio Interactions and Exposure Conditions. *Small* **2020**, *16*, No. 1907690.
(42) Wu, C.-Y.; Tu, K.-J.; Deng, J.-P.; Lo, Y.-S.; Wu, C.-H.; et al. Markedly Enhanced Surface Hydroxyl Groups of TiO2 Nanoparticles with Superior Water-Dispersibility for Photocatalysis. *Materials (Basel)* **2017**, *10* (5), No. 566.
(43) Bar-Ilan, O.; Louis, K. M.; Yang, S. P.; Pedersen, J. A.; Hamers, R. J.; Peterson, R. E.; Heideman, W. Titanium dioxide nanoparticles produce phototoxicity in the developing zebrafish. *Nanotoxicology* **2012**, *6*, 670−679.
(44) Lin, S.; Yu, T.; Yu, Z.; Hu, X.; Yin, D. Nanomaterials Safer-by-Design: An Environmental Safety Perspective. *Adv. Mater.* **2018**, *30*, No. e1705691.
(45) Yan, L.; Zhao, F.; Wang, J.; Zu, Y.; Gu, Z.; Zhao, Y. *Adv. Mater.* **2019**, *31*, No. 1805391.

https://doi.org/10.1021/acsomega.3c00734
ACS Omega 2023, 8, 18743−18750